Low Temperature Plasma Technology Laboratory

Density jump in helicon discharges

Francis F. Chen and Humberto Torreblanca

LTP-702   February, 2007

LTPTL

Electrical Engineering Department
Los Angeles, California 90095-1594

UNIVERSITY OF CALIFORNIA   •   LOS ANGELES

Density jump in helicon discharges

Francis F. Chen* and Humberto Torreblanca[†]
University of California, Los Angeles, California 90095-1594

ABSTRACT

Helicon discharges characteristically exhibit a sharp jump from low to high density as the radiofrequency (RF) power is raised. This is usually explained by the transition from an inductively coupled plasma (ICP) mode to a helicon mode when the dispersion relation for helicon wave propagation is satisfied at a critical power or magnetic field. Experiments have suggested a different mechanism for the sudden jump, a mechanism that depends on overcoming the parasitic circuit losses. This effect is analyzed computationally, and agreement with measurements is obtained.

In most helicon experiments the plasma density n changes abruptly as the RF power or magnetic field **B** is raised. This behavior was explained by Ellingboe and Boswell[1] as transitions from capacitive to inductive coupling, and subsequently into various radial helicon modes. A detailed analysis of transitions between different inductive and helicon modes was first given by Shamrai[2]. Recently, Lee et al.[3] have measured the electron energy distribution functions in the ICP and helicon modes and found differences that lead to hysteresis behavior when the power is cycled. In experiments on an eight-tube array of helicon sources[4], the jump to high density occurs in one tube at a time, and the magnitude of the jump can be explained by a slightly different mechanism which depends on overcoming the circuit losses. It was this behavior of the multiple-tube system that led to consideration of the circuit losses. The calculations given here apply to single tubes and are not limited to the experiment on which the effect was detected. Similar results would apply to other helicon discharges but may not be dominant there. This idea therefore complements previous concepts and does not contradict them.

The helicon sources operate in the low-field mode[5], in which the plasma resistance R varies non-monotonically with either B or n. This behavior arises from constructive interference of the reflected back wave at resonant conditions, and $R_p(n)$ can be computed in the uniform-*B* approximation by the HELIC code of Arnush[6]. An example is shown in Fig. 1 for three values of **B**. Subsequently, **B** = 80G will be assumed. In these calculations, the parameters are those of the experiment: plasma radius a = 2.5 cm, tube length L = 5 cm, antenna radius 3.7 cm, RF frequency 13.56 MHz, pressure 20 mTorr of Ar. The plasma from each tube is injected into a large chamber. The antenna is an azimuthally symmetric (m = 0) three-turn loop placed at the bottom of the tube near the entrance to the chamber[4]. The power P_{rf} from the power supply is fed to a matching network and then connected in parallel to the eight tubes. The *B*-field, from permanent magnets, is non-uniform, varying between the values in Fig. 1 along the tube length.

The cables, connectors, and match circuit have an unavoidable resistance R_c. The power deposited into the plasma, P_{in}, is related to P_{rf} by
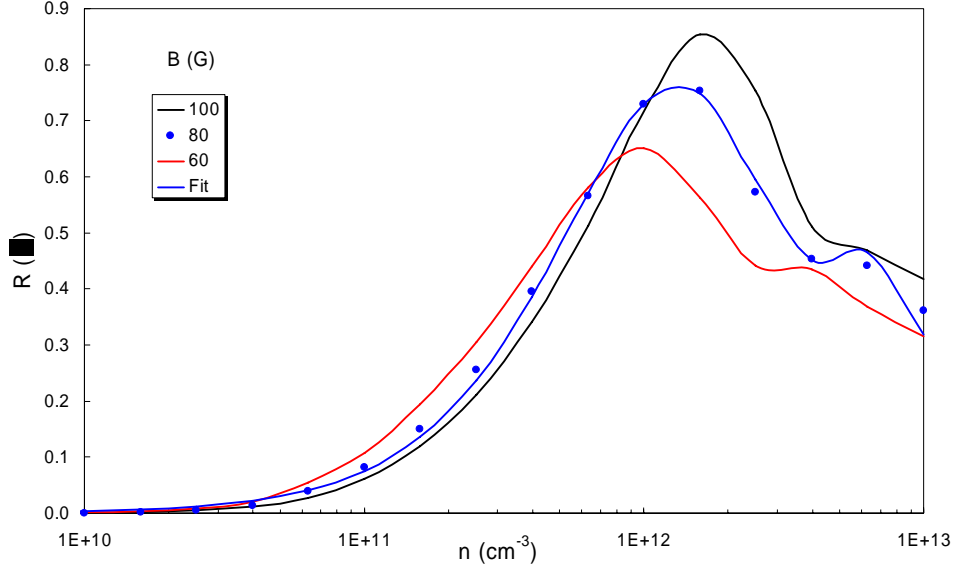
$$P_{in} = P_{rf} \frac{R_p}{R_p + R_c}.$$

(1)

Fig. 1. Plasma resistance R_p vs. ln(n) for three values of B. For 80G, the line is an analytic fit to the computed points.

The aim is to make $R_p \gg R_c$ so that $P_{in} \approx P_{rf}$, but this is not possible at low power and low density. Power balance is illustrated qualitatively in two limits. (Henceforth P_{in}, P_{rf}, R_p, and R_c will refer to that in *each tube*). In the limit $R_p \ll R_c$, P_{in} will be proportional to R_p. This case is illustrated in Fig. 2, where the 80-G R_p curve of Fig. 1 is shown on a log scale on the right-hand side. The power into the plasma, P_{in}, is shown as the upper solid curve (left-hand scale), as computed from Eq.(1) for $R_c = 10\Omega$ and 500W of P_{rf}. Since $R_p \ll R_c$, the P_{in} curve has almost the same shape as the R_p curve. The power lost by the plasma will be proportional to n and is represented by the dashed line, which will be explained in detail later. Power balance is possible at two densities, $\sim 6 \times 10^{10}$ cm^{-3} and $\sim 1 \times 10^{12}$ cm^{-3}. This mode is not the B = 0 ICP mode, whose P_{in} is shown in Fig. 2 as the dot-dash line. The lower intersection is a helicon mode with finite B and should be unstable, as explained by Shamrai[2]. The ICP mode for this set of conditions has only one intersection, but the mode does not exist at 80G. As seen from the lowest (dotted) curve in Fig. 2, the plasma resistance R_p is lower for the ICP mode than for the helicon mode at high densities but is higher at lower densities. This is shown for comparison only, since the two modes refer to different B-fields.

In the opposite limit $R_p \gg R_c$, P_{in} is no longer proportional to R_p, and the curve changes shape, according to Eq. (1). For instance, for $R_c = 0.1\Omega$, the P_{in} curves at various P_{rf} are shown in Fig. 3. We see that P_{in} is almost equal to P_{rf} at high density. The loss line is computed from[7,8]

$$W = E_c + W_i + W_e, \tag{2}$$

where W_i and W_e are the ion and electron energies carried out to the walls, and E_c is the energy lost to radiation in each ionization, as computed by Vahedi[9] and quoted by Lieberman and Lichtenberg[7]. For $T_e = 3$eV and $p = 20$mTorr, the approximate value is

$$P_{out} \approx 3.1 \times 10^{-11} n \text{ Watts} . \tag{3}$$

We see that energy balance is achieved at a high density increasing roughly linearly with P_{rf}. For larger circuit losses, $R_c = 0.5\Omega$, the situation is shown in Fig. 4. Here P_{in} does not reach a saturated value and is much lower than the applied power P_{rf}. There is no solution for $P_{rf} \leq$ 20W. For $R_c = 1.0\Omega$, the curves are similar but are lower still. Note that the density achieved

with helicons is only about 50% higher than with an ICP at 400W. This margin is even smaller at smaller R_c. The order-of-magnitude higher densities are attained only in the "big blue mode", which is caused by positive feedback between KT_e and neutral depletion. For uniform plasmas, the advantage of helicons lies in the higher values of R_p when R_c is not negligible. This advantage is more apparent with more efficient antennas than the single-loop, $m = 0$ antennas used here.
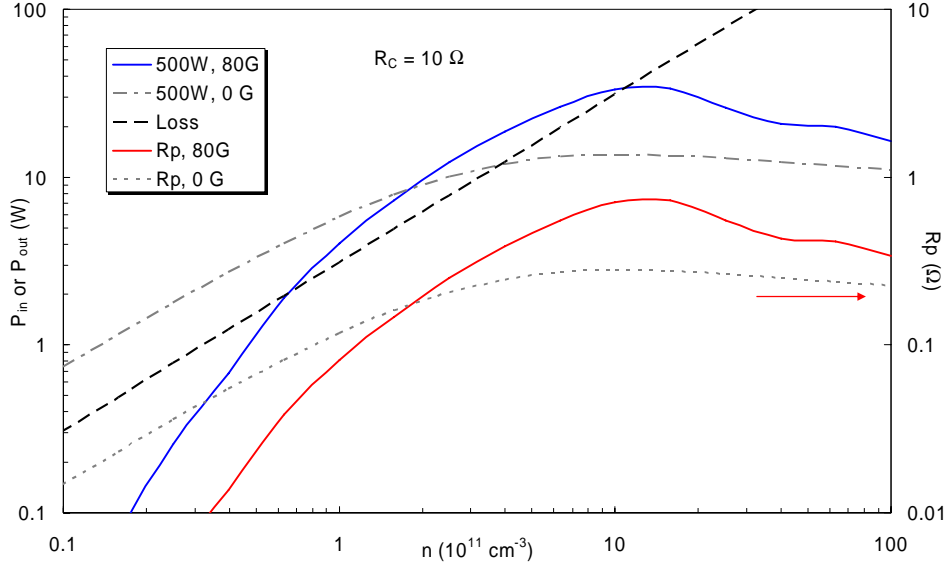

Fig. 2. Plasma input power P_{in} (—— , l.h. scale) and resistance R_p (—— , r.h. scale) vs. density n at 80G, $R_c = 10\Omega$, and $P_{rf} = 80$W. The dashed line (- - -,l.h. scale) is the power out of the plasma. The dot-dash line ($\cdot$ — $\cdot$ —, l.h scale) is P_{in} for the $B = 0$ ICP mode, and the dotted line ($\cdots\cdots$, r.h. scale) is its R_p computed with HELIC.
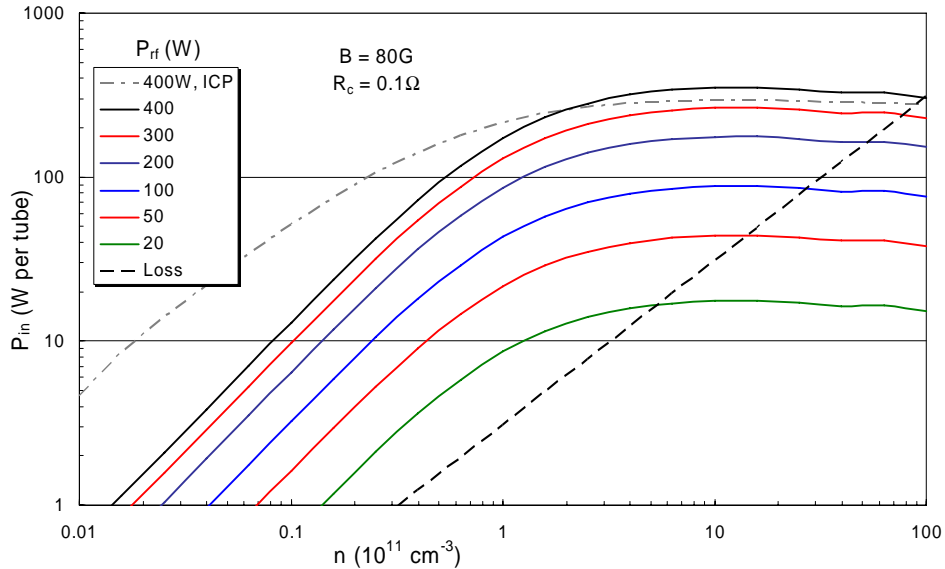

Fig. 3. Power absorbed into the plasma vs. density for $R_c = 0.1\Omega$ and various P_{rf}. The curves are in the same order as in the legend (color online). The straight line approximates the plasma losses, and the dot-dash line is the ICP result at $B = 0$.
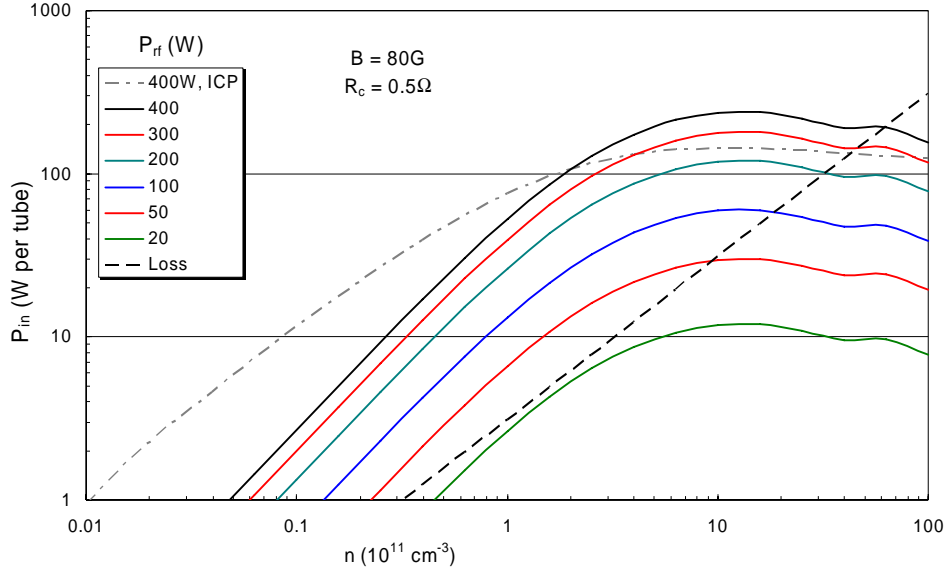
Fig. 4. Same as Fig. 3 but for $R_c = 0.5\Omega$.

Since R_p is a computed function of n, the equilibrium density at each P_{rf} can be obtained by solving Eqs. (1) and (3) simultaneously. For this purpose, the R_p curves of Fig. 1 can be fitted by an analytic function of the form

$$R = an^b e^{-cn} + d*[e^{-[(n-f)/g]^2} - d^{(f/g)^2}],$$ (4)

where $a, b, c, d, f,$ and g are adjustable constants. The fit for 80G was shown in Fig. 1. The computed density achieved as the power applied to each tube is increased is shown in Fig. 5. It is clear that an abrupt jump into the high-density mode occurs at a critical P_{rf} (P_{crit}) which depends on R_c. Below the critical P_{rf} there is actually no solution in the calculation although a dim discharge is always seen in the experiment. This is easily explained by the inaccuracy of the R_p calculation, which does not account for capacitive coupling, the B-field nonuniformity, and other effects, and of the approximate fit to the computed points.

The magnitude of P_{crit} has been checked experimentally. When P_{rf} is raised in the eight-tube source, first one tube jumps into the bright mode at the power at which the P_{in} curve is just tangent to the loss curve (Fig. 4). This is the tube that has slightly better antenna coupling or matching than the others. This tube then receives most of the power while the other tubes flicker unstably so that good RF matching cannot be attained. At a power sufficient to bring two tubes into high-density operation, another tube jumps to high density, and so on until all eight tubes are equally bright and reflected power can be brought to zero. Once all are in the high-density mode, it is seen from Fig. 5 that n is insensitive to small variations in P_{rf} to each tube. It is observed that ~40W per tube is required to light the first tube if $R_c = 1\Omega$. As also shown in Fig. 5, this is in agreement with Langmuir probe measurements of the density on axis inside the discharge tube near the plane of the antenna. Though it was not possible to measure R_c directly, its magnitude could be estimated from a program that calculates the capacitances C_1 and C_2 of the matching circuit for given load resistance R, inductance L, and cable length. With measured C_1 and C_2, it was then possible to solve for R and L. Operating at low power so that R_p is negligible, we found that $R_c \approx 0.7\Omega$ and $L \approx 0.8$ μH per tube. This is in rough agreement with the measured jump in density in Fig. 5. At high power, measurements of C_1 and C_2 with eight
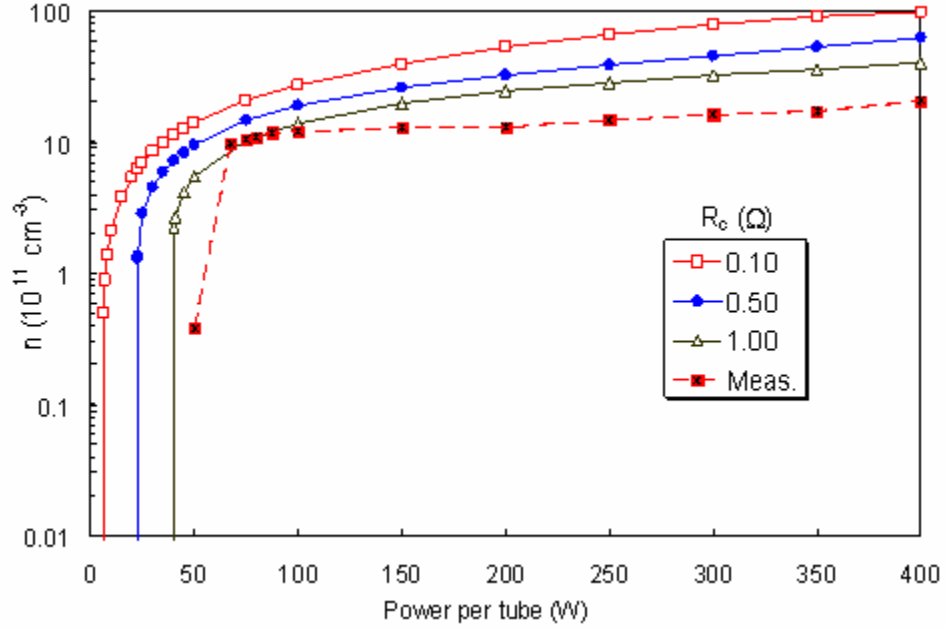
Fig. 5. Density vs. P_{rf} for three values of circuit resistance R_c, showing the abrupt jump in density as applied power is increased. The dashed curve shows density measured inside the discharge tube.

tubes running at 400W per tube show that $R = R_c + R_p \approx 3\Omega$ per tube. If R_c is $\leq 1\Omega$, R_p must be $\geq 2\Omega$ per tube, which is larger than what computations predict. In an attempt to reduce R_c, a new transmission line was designed in which and effective cable length to each antenna was different. Each antenna was not matched exactly, but the total array was matched. In this case R could not be measured; but the tubes, though connected differently, could be brought to the same brightness by virtue of the flatness of the curves on Fig. 5, showing that n is insensitive to small variations in R_c or P_{in}.

The absolute magnitude of the measured density in Fig. 5 agrees amazingly well with that calculated for high powers, considering the approximations in the theory. There were no adjustable parameters. The measured density was lower, probably due to neutral depletion, which is not taken into account in HELIC. We have checked that R_p, as calculated by HELIC, is insensitive to the radial density profile assumed. It is sensitive to the antenna radius, but this can be measured accurately enough. The largest source of error is in the calculation of plasma losses. In applying Eq. (2) we assumed classical diffusion, whereas the transport could be anomalous. Furthermore, the variation in magnetic field and plasma radius within the tube were neglected, as well as neutral depletion there.

If the magnetic field is removed, stable discharges can be obtained in all eight tubes of our device without a violent jump. This is the ICP mode shown in Fig. 2. Note that it has a much higher R_p than the helicon mode before the jump, and hence much higher n when $R_c >> R_p$. After the jump, the helicon's R_p is larger by a factor 2.7 (at 80G). If R_c is still $>> R_p$, the density of a helicon discharge is only 2.7 times larger than that of an ICP discharge. However, since the ICP's R_p is limited to 0.3Ω, it is easier to achieve $R_p >> R_c$ with helicons. At higher B-fields, the helicon's R_p is higher and occurs at higher n (Fig. 1). The condition $R_p >> R_c$ can be obtained by increasing n with higher P_{rf}. Then the circuit losses can become negligible, a condition difficult to achieve for an ICP, at least in small tubes.

Summary

Calculations using the HELIC program[6] predict a sudden jump into a high-density helicon mode at a threshold RF power which depends on the ratio of plasma loading resistance to circuit resistance. The threshold power and plasma density measured experimentally agree quantitatively with the predictions. Although the experiment was a multi-tube system, the theory and analysis relate to a single-tube discharge. It was the behavior of the multi-tube system that elucidated the mechanism that causes abrupt density jumps. The numerical values depend on discharge parameters such as the tube size, antenna design, and RF frequency, but the effect of circuit resistance on density jumps should be relevant to any discharge where the loading resistance is not monotonic and very high.

Calculations do not predict a low-density discharge at low power, but one is seen. This is not an ICP discharge, since the finite magnetic field precludes that mode in our system. The faint discharge may be capacitively coupled, but it does not appear to be asymmetric due to our tightly wound $m = 0$ antennas. It could also be a low-density helicon mode. Its nature is not known, but the observed jump is *not* from an ICP mode into a helicon mode. Calculations with $B = 0$ for the same geometry show that ICP operation suffers little in comparison with low-field helicon operation. The difference is in the higher loading resistance achievable with helicons, which enables them to overcome circuit losses more easily. The difference comes down to the RF absorption mechanism, which in helicon discharges is dominated by coupling to the rapidly damped Trivelpiece-Gould modes, a magnetic field effect not available in ICPs.

For sufficiently large R_p, the plasma density after the jump is insensitive to small variations in RF coupling. This makes possible uniform power coupling from a single matching network to multiple tubes at varying distances.

REFERENCES

* ffchen@ee.ucla.edu

† ht@ucla.edu

1 A.R. Ellingboe and R.W. Boswell, Phys. Plasmas **3**, 2797 (1996).

2 K. P. Shamrai, Plasma Sources Sci. Technol. 7, 499 (1998).

3 M.H. Lee, K.H. Lee, D.S. Hyun, and C.W. Chung, Appl. Phys. Lett. **90**, 191502 (2007).

4 F.F. Chen and H. Torreblanca, Plasma Phys. Control. Fusion 49, A81 (2007).

5 F.F. Chen, Phys. Plasmas **10**, 2586 (2003).

6 D. Arnush, Phys. Plasmas **7**, 3042 (2000).

7 M.A. Lieberman and A. J. Lichtenberg, *Principles of Plasma Discharges and Materials Processing* (Wiley, New York, (1994), 2nd ed., p. 333.

8 F.F. Chen and J.P. Chang, *Principles of Plasma Processing* (Kluwer/Plenum, New York, 2002), p. 71.

9 V. Vahedi, *Modeling and simulation of RF discharges used for plasma processing*, Thesis, University of California, Berkeley (1993).